

Improvements in the simulation of liquid fuel combustion in a low-temperature fluidized bed

MICCIO Michele

mmiccio@unisa.it

FERRANTE Lorenzo

lferrante@unisa.it

Dip. di Ingegneria Chimica ed Alimentare, Università di Salerno

Via Ponte don Melillo - 84084 FISCIANO SA

Italy

FARAVELLI Tiziano

tiziano.faravelli@polimi.it

FRASSOLDATI Alessio

alessio.frassoldati@polimi.it

RANZI Eliseo

eliseo.ranzi@polimi.it

Dip. di Chimica, Materiali ed Ingegneria Chimica "Giulio Natta", Politecnico di Milano

Piazza Leonardo da Vinci, 32 - 20133 MILANO MI

Italy

The paper presents a further work along the route towards a more thorough description of fundamentals and mechanisms governing the liquid fuel combustion in bubbling fluidized bed combustors (FBC), operating in a temperature range (i.e., 650-800°C) that is lower than the classical value for FBC of solid fuels. Three new sub-models have been added to an existing “system model”: i) formation of a reacting gas-liquid flare inside the bed downstream from the liquid fuel nozzle; ii) motion and coalescence of the fuel vapor bubbles; iii) mixing and combustion in the *splash zone*.

Among the other things, the simulation code predicts temperature and concentration of the unburned species and combustion products inside the bed, bubbles and splash zone.

1. Introduction

Faravelli and coworkers originally published in 2003 a “system model” for the homogeneous combustion of hydrocarbon liquid fuels on the basis of a detailed chemical kinetics scheme in a low-temperature bubbling fluidized combustor. Later on, Ferrante and Miccio (2006) presented an adaptation of that model to simplified bed operating conditions, i.e., at minimum fluidization. They aimed at improving the significance of the model by taking advantage of measurements that were purposely carried out in experiments on a pre-pilot combustor.

Three new sub-models have been developed and are considered in the present work.

First, a Sub-model of a horizontal gas-liquid jet entering the fluidized bed downstream of the fuel nozzle has been developed. It follows the pseudo-fluid model by Ariyapadi et al. (2003) (i.e., an evolution of the original model by De Michele et al., 1976); in addition, it considers liquid vaporization (as already partially done by Zhu et al., 2001), the eventual conversion of the vaporized species by pyrolysis and oxidation in the gas phase and, finally, the generation of an endogenous (i.e., containing fuel vapors and/or pyrolysis products) bubble. The main assumptions are: i) the jet is at steady-state; ii) the slip velocity between the three phases (atomization gas, liquid droplets, entrained solid particles) is negligible; iii) on a given jet cross section, concentrations and temperature

of all three phases are uniform; iv) the pressure is constant along the jet; v) the jet is divided in two main regions: initial zone and fully developed region; vi) a new endogenous bubble detaches from the flare with a generation frequency $f_{b0} = 6$ Hz and an initial diameter $D_{b0} = 5$ cm, as suggested by Ferrante (2007) after a comparison with experimental results. Basically, the Sub-model performs balances of mass, momentum and enthalpy along the jet axis. Equations and details are reported in Ferrante (2007). Second, a Sub-model of bubble coalescence according to the concept of “bubbles train” has been developed and embodied in the main model that was already available (Faravelli et al., 2003) to handle fluid dynamics, mass and heat transfer, and chemical reactions in the fluidized bed. The main focus of the present paper will be just on the description of this upgraded model and the discussion of the new results generated by it. Third, a Sub-model of the splash zone has been developed by adopting the Pemberton and Davidson (1984) theory of the “ghost bubble”: hence, the bubble erupting at the bed surface retains its identity in the splash zone. The main assumptions are: i) the splash region is made of two phases, i.e. ghost bubble and external gas phases; ii) the ghost bubble is a spherical, homogeneous and well mixed entity; iii) the bubble volume increases with the height, whereas its velocity decreases; iv) the external phase is perfectly mixed. Basically, the Sub-model performs mass and energy balances on both the phases in the splash region. Equations and details are reported in Ferrante (2007). All in all, the new Sub-models allow to overcome the previous model limits, which were due to the use of uncertain or adjustable parameters, and to achieve a further progress in the model predicting capacity.

2. Mathematical Model of the Bubbling Bed Reactor

2.1. Fuel Bubble Sub-model

The new Sub-model describing the bubbling bed fluid dynamics considers each bubble inserted in a train of rising bubbles. Under such circumstances the individual bubble rise velocity changes because of wake effects and becomes a nonlinear relationship that couples the rise velocity and motion of a given bubble to the motion of its neighbors. The interactions affect each individual bubble and often result in coalescence. The above approach is similar to that proposed by Daw e Hallow (1992) and Farrokhlaee (1970), who already proved that the resulting model is capable to describe the chaotic behavior of the bubble phase in gas fluidized beds.

The following key assumptions are made: i) the fraction of liquid fuel vaporized inside the flare and the initial composition of the fuel bubble are obtained by the jet sub-model; ii) the fuel bubble rises along the bed as a spherical, homogeneous and well mixed entity and undergoes mass and energy exchange with the emulsion phase according to conventional approach; iii) each fuel bubble – let’s say the j -th bubble - rising the bed in a train of fuel bubbles is traced individually up to the bed outlet or the point of a possible coalescence act; iv) when coalescence of two bubbles occurs, merging of their masses and energy exchange are instantaneous.

For the j -th fuel bubble the equation of motion, the mass balance of i -th species and the energy balance are, respectively:

$$\frac{dz_j}{dt} = U_{br} \left\{ 1 + 3 \left[D_{bj-1} / (z_{j-1} - z_j) \right]^3 \right\} \quad (1.)$$

$$\begin{aligned} \frac{dm_{i,j}}{dt} = & k_{\omega,i,j} \cdot (\omega_{i,e} - \omega_{i,j}) \cdot S_{b,j}(t) + R_{i,j} \cdot V_{b,j}(t) \cdot PM_i + \\ & + \delta(\theta_{j+1}) \cdot V_{b,j+1}(\theta_{j+1}) \cdot \omega_{i,j+1} \cdot \rho_{j+1} \end{aligned} \quad (2.)$$

$$\begin{aligned} \sum_i m_{i,j} \cdot c_{vi,j} \cdot \frac{dT_j}{dt} = & \sum_i k_{\omega,i,j} \cdot (\omega_{i,e} - \omega_{i,j}) \cdot (u_{i,e} - u_{i,j}) \cdot S_{b,j} - \\ & - \sum_i u_{i,j} \cdot R_{i,j} \cdot V_{b,j} \cdot PM_i + \delta(\theta_{j+1}) \cdot V_{b,j+1}(\theta_{j+1}) \cdot \omega_{i,j+1} \cdot \rho_{j+1} \cdot u_{i,j+1} \end{aligned} \quad (3.)$$

where j is a bubble index counting from top to down; U_{br} = lone bubble rise velocity [m/s]; $m_{i,j}$ = mass the i -th species in the j -th bubble [kg]; $k_{\omega,i,j}$ = mass transfer coefficient of i -th species between the j -th bubble and the emulsion [kg/m²/s]; $\omega_{i,e}$, $\omega_{i,j}$ = mass fractions of i -th species in the emulsion phase and in the j -th fuel bubble; $R_{i,j}$ = reaction rate of i -th species in the j -th bubble [kmol/m³/s]; $S_{b,j}(t)$ = surface of the j -th bubble [m²]; $V_{b,j}(t)$ = volume of the j -th bubble [m³]; T_j = temperature of the j -th bubble [K].

The eq.1 relates the rise velocity of a given bubble to the distance from the preceding one; therefore, a lower bubble can have a higher velocity than the upper one and in principle can reach it during their rise along the bed.

The above eqs. are written for each fuel bubble and hold as long as the j -th bubble keeps its identity in the bed, i.e., $(z_{j-1} - z_j) - \frac{(D_{bj-1} + D_{bj})}{2} \geq 0$. $\delta(\theta_{j+1})$ [s⁻¹] is the Dirac function and θ_{j+1} is the time instant, if any, at which the coalescence for the $(j+1)$ -th trailing bubble condition occurs, i.e., $(z_j - z_{j+1}) - \frac{(D_{bj} + D_{bj+1})}{2} < 0$.

Because of the periodic generation past the jet flare, coalescence in the bed and eruption at the bed surface, the total number of bubbles $N(t)$ inside the bed is not constant over the time. The topmost bubble leaves the bed when its centre reaches the bed surface: as a consequence $N(t)$ is reduced by 1 at that time. Again, when the $(j+1)$ -th trailing bubble coalescences with the j -th leading bubble, $N(t)$ is reduced by 1. On the other side, $N(t)$ is increased by 1 at the time a new endogenous bubble is generated by detachment from the jet flare.

2.2. Sub-model of the dense phase

A quasi-steady state mass balance can be written for each i -th species:

$$G_{mf} \omega_{i,mf} + \sum_j G_{i,j} + \chi R_i W_i V_{bed} \varepsilon_{mf} (1 - \varepsilon_b) = G_{out} \omega_{i,e} \quad (4.)$$

$$\text{where } G_{i,j} = k_{\omega,i}^f (\omega_{i,j} - \omega_{i,e}) S_{b,j}; \quad G_{out} = \sum_j \sum_i G_{i,j} + G_{mf} \quad (5.)$$

and χ is a reducing factor that accounts for the wall termination effect on free radicals.

2.3. Model solution and integration

All in all, the bubbles and bed sub-models are composed of $(M \times N)$ material balance equations, N energy balance equations and N equations relative to the vertical position of the fuel bubbles. The resulting ODE system is not of constant order during time. Appropriate initial conditions are associated.

All the new sub-models have been fully integrated into the original FORTRAN code.

As a first step, the program solves the equations relative to the sub-model of jet flare. This sub-model gives as output the initial composition of the bubble generated at the bottom of the bed, and the fraction of the fuel directly fed to the emulsion phase. Those parameters are utilized as input in the bubbles and bed model.

The BzzOde module, i.e., a C++ code for the solution of stiff and non-stiff ODE's (Buzzi and Manca, 1998), has been linked to the main FORTRAN code.

After integration in the time domain, the code saves as output data the temperature profiles and the concentration history of about 250 species in the jet flare, fuel bubbles, emulsion phase and splash zone, respectively.

3. Results and Discussion

The model calculations were arranged so as to consider a base case for the FRB140 reactor fired with n-dodecane, run at steady state with an overall excess air factor, $\lambda=1.29$ and at minimum fluidization (Ferrante and Miccio, 2006). The temperature of the emulsion phase, T_e , was set at 650, 700, 750 and 800°C.

Table 1: Time-averaged compositions of the main chemical species in the simulation (fuel n-dodecane, $T_e=650^\circ\text{C}$, $d_{b0}=5\text{ cm}$, $u_0=100\text{ m/s}$)

| Species | Initial bubble composition (mol. frac.) | Emulsion phase (mol. frac.) | Bubble at bed outlet (mol. frac.) | “Ghost bubble” at exit of splash zone (mol. frac.) |
|-----------------------------------|---|-----------------------------|-----------------------------------|--|
| N₂ | 7.60E-01 | 7.50E-01 | 7.26E-01 | 7.44E-01 |
| H₂ | 1.53E-03 | 1.67E-02 | 2.19E-02 | 2.49E-03 |
| O₂ | 2.00E-01 | 7.98E-02 | 8.23E-02 | 2.01E-02 |
| H₂O | 8.41E-04 | 5.36E-02 | 6.23E-02 | 1.06E-01 |
| CO₂ | 3.01E-04 | 8.44E-02 | 3.68E-02 | 1.03E-01 |
| CO | 1.52E-08 | 9.55E-03 | 6.00E-02 | 1.41E-02 |
| H₂O₂ | 1.81E-17 | 1.51E-04 | 3.56E-04 | 8.56E-08 |
| CH₄ | 1.12E-05 | 5.36E-04 | 5.84E-03 | 4.75E-08 |
| C₂H₄ | 4.98E-07 | 1.15E-03 | 1.80E-03 | 6.20E-08 |
| C₂H₂ | 2.89E-06 | 2.50E-05 | 8.85E-06 | 1.05E-07 |
| n-C₁₂ | 3.66E-02 | 6.01E-04 | 3.77E-05 | 8.13E-13 |

Table 1 is a synthetic picture of one of the model capabilities. It reports the time-averaged compositions of the main chemical species as calculated by the model for the above mentioned reference case at $T_e = 650^\circ\text{C}$. As far as the initial composition of the

endogenous bubble, it is clear that the bubble is still mainly composed of oxygen, nitrogen and n-dodecane, being the low temperature oxidation mechanism inhibited by the quenching effect due to the fuel evaporation. The bubble at bed outlet has a higher composition in the final oxidation products (e.g., CO_2 and H_2O), but it still presents a relatively large concentration of reaction intermediates (e.g., H_2O_2) and pyrolysis products (e.g., CH_4 and C_2H_4). Of course, the “ghost bubble” at exit of splash zone is characterized by a further growth of the final oxidation products and a depletion of reaction intermediates, pyrolysis products as well as oxygen. In general, the emulsion phase composition is not much different from the bubble composition at bed outlet; the n- C_{12} concentration turns out relatively high because of the large fraction of fuel entering the emulsion phase still in liquid state when $T_e=650^\circ\text{C}$.

A better understanding of the fuel conversion in a low temperature bed ($T_e=923\text{ K}$) at minimum fluidization can be achieved by following the evolution of the endogenous bubble by means of the model calculations.

Fig. 1 reports the temperature (Fig. 1C) and species evolution (Fig. 1A-B) as they come out from a typical simulation when a fuel bubble travels through the emulsion phase

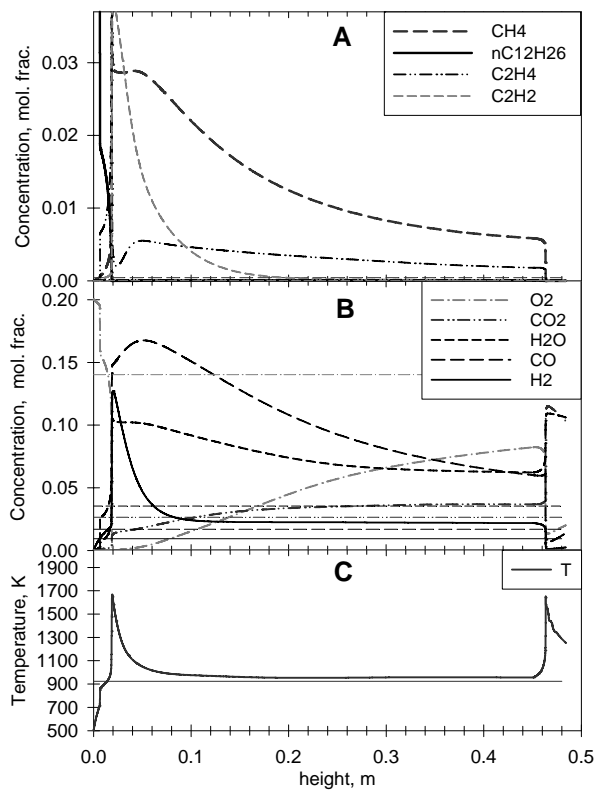


Figure 1: Temperature and main composition profiles of an endogenous bubble rising without any coalescence. Horizontal lines refer to the time-averaged compositions in the emulsion phase at $T_e=923\text{ K}$. Fuel n-dodecane. Bubble initial conditions: $d_{b0}=5\text{ cm}$, $u_0=100\text{ m/s}$.

without coalescence and, later on, through the splash region. The time-averaged species concentrations of the emulsion phase are reported as horizontal lines in the same Fig. 1.

The following features can be singled out:

The sudden temperature rise from 750 K to 900 K at $z=0.01\text{ m}$ is the effect of the low temperature oxidation mechanism. At about 900 K the peroxy radicals become unstable and the reactivity of the system declines. This fact is well evident in Fig. 1B, where the O_2 profile shows a very sharp drop from about 0.20 to 0.17. It is possible to observe the high temperature ignition delay at about 0.02 m where the temperature peaks up to about 1700 K and where CO, H_2 and acetylene formation sharply increases. This hot ignition is

controlled by the total amount of oxygen inside the bubble and limitation to its diffusion from the emulsion phase.

From $z=0.02$ to 0.06 m the CO, CH₄ and C₂H₄ concentrations increase, this finding being due to the progressive decomposition of the heavier hydrocarbons (e.g., C₂H₂) formed from fuel pyrolysis and not completely converted in the first hot ignition. The temperature suddenly decreases.

From $z=0.06$ m to the bed exit the high temperature mechanism mainly controls the methane and ethylene gradual decrease, together with heavier olefins, and forms CO₂ and H₂O. This conversion keeps the temperature above that of the emulsion, T_e, but the reaction of conversion of the hydrocarbon species are low and so the O₂ starts accumulating into the bubble.

Once reached the bed exit, at a height $z=0.45$ m, the bubble erupts into the splash region. The bubble composition is rich of oxygen, which has been accumulated in the bubble during the rise of the last part of the bed, and of hydrocarbons and CO still unconverted. In this region the bubble is not quenched by the emulsion phase anymore, so its temperature progressively increases up to about 1100K and at this temperature the *ghost bubble* ignites. During this second ignition all the hydrocarbons and almost all the CO in the *ghost bubble* are converted.

The most important finding in the present simulation is that a second bubble ignition is observed in the splash region for a simulation at low bed temperature. This finding confirms that the model with the newly introduced sub-models is capable of predicting the occurrence of micro-explosions (Ferrante, 2007) at or just above the bed surface.

In the emulsion phase, which is characterized by a relatively low temperature, all the conversion and oxidation reactions are slow and the n-C₁₂ decomposition is limited, in spite of the large amount of n-C₁₂ fed to the emulsion (the fraction of fuel vaporized in the flare is only 63% in the present simulation).

4. References

- Ariyapadi S., Berruti F., Briens C., Griffith P and Hulet C. (2003), The Canadian Journal of Chemical Engineering, **81**.
- Buzzi Ferraris G. and D. Manca (1998), Comp. & Chem. Eng., **22**, p. 1595-1621
- Daw C.S. and Hallow J.S. (1992), AIChE symp. Series, **88**, No. 289.
- De Michele, G., A. Elia and L. Massimilla (1976), Ing. Chim. Ital., **12**, p. 155-162.
- Faravelli T., Frassoldati A., Miccio F., Miccio M. and Ranzi E. (2003), Paper FBC2003-133, Proc. of 17th Int. Conf. on Fluidized Bed Combustion, Jacksonville, Florida (USA), published on CD-ROM by ASME, ISBN 0-7918-3675-4.
- Farrokhlaee T. and Clift R. (1980), Proc. of the 1980 International Fluidization Conference, Henniker, New Hampshire, p.135-142.
- Ferrante (2007), Ph.D. Thesis in Chemical Engineering, Univ. of Salerno
- Ferrante L. and Miccio M. (2006), Paper 93.I, Proc. of 19th International Conference on Fluidized Bed Combustion, ISBN 3-200-00645-5, Vienna (A), May 21-24,
- Pemberton, S. T. and Davidson J. F. (1984), Chem. Eng. Sci., **39**, 829.
- Zhu C., Fan L.-S., Lau R., Vuong K., Warsito W., Wang X., Liu G. (2001), Chemical Engineering Science, **56**, p. 5871–5891